Waveguide tapering for improved parametric amplification in integrated nonlinear Si3N4 waveguides

Research Article | Vol. 28, No. 16 / 3 August 2020 / Optics Express 23467
Optics EXPRESS

Waveguide tapering for improved parametric amplification in integrated nonlinear Si_3N_4 waveguides

PING ZHAO,* ZHICHAO YE, KOVENDHAN VIJAYAN, CORENTIN NAVEAU, JOCHEN SCHRÖDER, MAGNUS KARLSSON, AND PETER A. ANDREKSON

Photonics Laboratory, Department of Microtechnology and Nanoscience, Chalmers University of Technology, SE-412 96 Gothenburg, Sweden
*pingz@chalmers.se

Abstract: In this paper, we propose and numerically investigate waveguide tapering to improve optical parametric amplification in integrated nonlinear Si_3N_4 circuits. The phase matching condition of parametric amplification changes along the length of uniform Si_3N_4 waveguides, due to the non-negligible propagation loss, potentially causing peak-gain wavelength shifts of more than 20 nm. By tapering the waveguide width along propagation, we can achieve a 2.5 dB higher maximum parametric gain thanks to the improved phase matching, which can also broaden the amplification bandwidth. Therefore, the length of an optimally tapered Si_3N_4 waveguide can be 23% shorter than a uniform one in the case of a 3.0 dB/m propagation loss and a single continuous-wavelength pump. Quasi-continuous tapers are efficient to approximate continuous ones and might simplify the fabrication of long tapered nonlinear Si_3N_4 waveguides, which are promising for optical signal processing and optical communications.

1. Introduction

Due to the advantages of broad optical bandwidth, flexible operation wavelength window and ultra-fast temporal response [1], optical parametric amplifiers (OPAs) based on third-order nonlinear effects in highly-nonlinear fibers (HNLFs) have been widely investigated and used in various areas including optical communications [2,3], optical signal processing [4,5], microwave photonics [6] and femtosecond lasers [7]. However, the polarization dependence of standard single-mode optical fibers is an issue for the practical implementation of fiber-based OPAs [8]. With the advance in nano-fabrication, more research is conducted on OPAs using integrated nonlinear photonic waveguides due to benefits from compactness, robustness and cost-efficient fabrication in large volumes [9–12]. A promising material platform is Si_3N_4, with appealing properties such as high third-order nonlinear coefficients [13], relatively low propagation loss (typically 3.0 dB/m [14–16]), negligible Raman and Brillouin scattering effects in a single-pass waveguide [17–19] and absence of two-photon absorption due to a large bandgap of ~5 eV. Moreover, since the absorption of Si_3N_4 at telecommunication band is extremely low [20] and the thermal-optical and thermal-expansion coefficients are small [21,22], the refractive index change as a result of thermal optical effects can be neglected and it has been demonstrated that nonlinear Si_3N_4 waveguides can support a 10 W continuous-wave (CW) laser power without material damage [23].

Generally, the typical propagation loss of a HNLF is about 0.8 dB/km and the pump attenuation in a hundreds-of-meter-long HNLF can therefore often be neglected. In contrast, the propagation loss of nonlinear Si_3N_4 waveguides still limits the parametric gain. To achieve efficient parametric gain with a CW pump required in optical communications, Si_3N_4 waveguides of several meter length will be needed. In this case, the attenuation of the pump during propagation has to be

#389159 https://doi.org/10.1364/OE.389159
Journal © 2020 Received 29 Jan 2020; revised 27 May 2020; accepted 30 May 2020; published 23 Jul 2020

Optics EXPRESS

accounted for [24], which affects the phase matching of parametric amplification. Engineering the waveguide geometry turns out to be an effective technique for improving nonlinear processes in optical waveguides. Using a tapered optical fiber to generate decreased group-velocity dispersion for efficient optical pulse compression was proposed in the 1980s [25]. Later, this approach was demonstrated experimentally in dispersion-decreasing tapered silica fibers [26] and theoretically investigated in silicon-based waveguides [27–29]. It has also been shown to broaden the bandwidth of third harmonic generation in fiber tapers [30]. Pulsed-pump phase-sensitive optical amplification in silicon waveguides with a short intermedium segment as a phase shifter was investigated in [31]. However, to achieve improved parametric amplification in the desired wavelength regime with CW pumping, the optimal design of integrated Si_3N_4 OPAs via tapering the waveguide has not been reported yet.

In this paper, we perform a systematic investigation of enhancing the broadband parametric amplification in Si_3N_4 waveguides with CW pumps by tapering the waveguide width to compensate for the degradation of phase match at the target signal wavelength. We propose a guideline on how to taper the width of Si_3N_4 waveguides for parametric amplification so that the peak-gain (PG) wavelength is maintained along the waveguide and verify performance by simulations. Due to the improved efficiency of the parametric process, the peak gain of a tapered Si_3N_4-waveguide OPA can be 2.5 dB higher than that of uniform waveguide according to the simulation results. Moreover, the bandwidth of the integrated Si_3N_4 OPA can be expanded with this technique. Therefore, to obtain the same maximum peak gain compared with a uniform Si_3N_4 waveguide OPA the tapered waveguide can be 25% shorter. Both increasing or decreasing the width of Si_3N_4 waveguide can be utilized to improve the parametric amplification. In addition, quasi-continuous tapers can operate efficiently, and this provides insights to the practical fabrication of long nonlinear Si_3N_4 waveguides which are promising in optical communications, optical signal processing and microwave photonics.

2. Principle

In this paper we investigate OPAs with a single CW pump. One signal wave (s) enters the nonlinear Si_3N_4 waveguide with one pump wave (p). Another wave, i.e. idler (i), is generated due to four-wave mixing in the waveguide [32]. The phase mismatch parameter κ of the OPA determines the strength of coupling between the three optical waves and is expressed as

$$\kappa = \Delta\beta + 2\gamma P_0 e^{-\alpha z} = \beta(\omega_s) + \beta(\omega_i) - 2\beta(\omega_p) + 2\gamma P_0 e^{-\alpha z} \quad (1)$$

where β is the propagation constant of the optical field in the waveguide, ω_k is the angular frequency of wave k in vacuum, α is the linear waveguide attenuation, γ is the nonlinear coefficient of the waveguide, z is the length of waveguide and P_0 is the input pump power. The linear phase mismatch $\Delta\beta \approx \beta_2\Delta\omega^2 + \beta_4\Delta\omega^4/12$, where $\Delta\omega = \omega_s$ - ω_p is the angular-frequency difference between the signal and the pump, and β_j (j = 2,3,4) are second-, third- and fourth-order dispersion coefficients at the pump wavelength. The maximum parametric gain occurs at the minimum absolute value of κ. It is clear that the nonlinear term ($\Delta\beta_R = -2\gamma P_0 e^{-\alpha z}$) of the phase mismatch changes with the length of the waveguide. The change can be neglected for short conventional HNLFs while it will affect the phase matching in nonlinear waveguides with significant losses such as Si_3N_4. Figure 1(a) shows the variation of $\Delta\beta_R$ (solid blue line) as a function of the length of a typical Si_3N_4 waveguide with α = 3.0 dB/m and γ = 1.0 $m^{-1}W^{-1}$. The input pump power P_0 is 35.4 dBm, which is chosen to get a net gain around 20 dB. The orange dashed line shows the decrease of pump power during propagation. It can be seen that the absolute value of $\Delta\beta_R$ drops as much as 86% after 3 m transmission. Figure 1(b) depicts the simulated gain spectra of Si_3N_4 OPAs with different lengths and the same uniform widths. Here the fundamental mode (TE_{00}) is used (the mode profile is shown by the inset). The waveguide has a Si_3N_4 core cladded by silica. The dimension of the core cross section is 1310 nm wide and 700 nm high. The refractive

Optics EXPRESS

index of Si_3N_4 and silica at 1550 nm wavelength is 1.990 and 1.443, respectively. The dispersion coefficients are calculated by COMSOL Multiphysics and used in all our OPA simulations which are based on numerically solving the nonlinear Schrödinger equation (NLSE) as

$$\frac{\partial A}{\partial z} + \frac{\alpha}{2}A - i\sum_{j=2}^{4}\frac{i^j\beta_j(z)}{j!}\frac{\partial^j A}{\partial T^j} = i\gamma|A|^2A \tag{2}$$

where A is the slowly varying envelope of the overall optical field and T is the relative time axis where a reference frame moves with the envelope at the group velocity [32]. The dispersion coefficients are allowed to vary with distance z and the dispersion of third and fourth orders is considered for wideband operation. As can be seen in Fig. 1(b), the PG wavelengths shift inward toward the pump when the length changes from 0.4 m to 3.0 m, due to the pump attenuation and the subsequent reduction in nonlinear phase-mismatch.

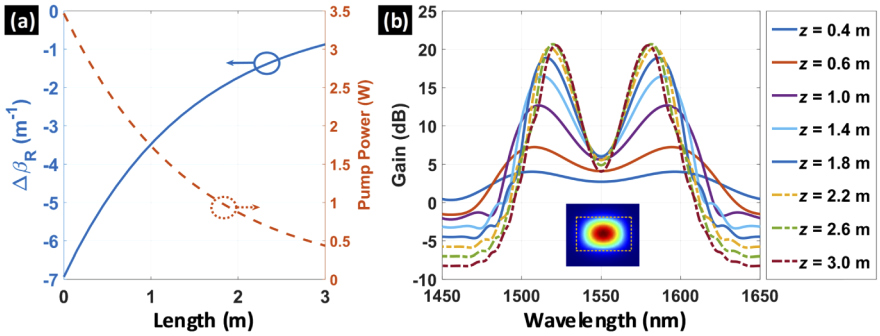

Fig. 1. (a) Required linear phase mismatch (solid blue line) and pump power (dashed orange line) varying with the length of a Si_3N_4 waveguide where $\kappa = 0$, $\alpha = 3.0$ dB/m, $\gamma = 1.0$ m^{-1}W^{-1} and $P_0 = 35.4$ dBm. (b) Simulated net gain spectra of uniform-width Si_3N_4-waveguide OPAs with different lengths. The inset is the mode profile of TE_{00} mode and the yellow dashed line is the boundary of the Si_3N_4 wavguide with a cross-section dimension of 1310 nm x 700 nm.

A method of improving the parametric amplification in Si_3N_4 waveguides is to taper the width (W) of the waveguide while maintaining the height (H). Figure 2(a) shows the calculated intrinsic $\Delta\beta$ of TE_{00} mode varying with the width of the Si_3N_4 waveguide with a height of 700 nm. The target PG wavelength is chosen to be 1600 nm and the pump is located at1550 nm. Letting $\Delta\beta = \Delta\beta_R$ for given γ, α and P_0, we calculate the continuous widths for different waveguide lengths to achieve peak parametric gain at the target 1600 nm signal wavelength. Figure 2(b) shows the calculated width along the Si_3N_4 waveguide with a propagation loss of 3.0 dB/m and input pump power of 35.4 dBm. The red line corresponds to the continuous taper. The difference between the widths at the two ends of the whole waveguide is 18 nm. Here, it is assumed that α and γ are constant along the waveguide for such a small width difference. To approximate the continuous long taper, several uniform segments with different widths and sub-milimeter-scale adiabatic tapers in between are used [33]. The length of each segment is equal. This can facilitate the fabrication of the tapered waveguides. Since the width difference between the two segements is less than tens of nanometer, the angles of these connecting adiabatic tapers are small enough so that reflections at the transition are neglected in all simulations. The width of each uniform segment is set to be the calculated value of width in the center of each segment. For example, the blue line in Fig. 2(b) shows the widths of ten uniform segments along the waveguide The first segment (# 1) is the widest and the tenth segment (# 10) is the narrowest. The calculated second-order dispersion curves of the ten uniform segments are depicted by Fig. 2(c). From the

Optics EXPRESS

first segment to the tenth segment, the local β_2 evolves almost parallelly to mitigate the increase of the absolute value of κ due to the loss of the 1550 nm pump for the target PG wavelength of 1600 nm. As can be seen, β_2 at 1550 nm wavelength is always negative and increases as the width decreases. Figure 2(d) shows the simulated gain spectra of three proposed tapered Si_3N_4-waveguide OPAs with lengths of 1.0 m (blue line), 2.0 m (red line) and 3.0 m (yellow line), respectively. Piecewise tapers with ten uniform segments are utilized in the simulation. A constant PG wavelength at 1600 nm is observed and shows the improved parametric amplification at the target wavelength when z is 3.0 m. To present a clear picture of our design, Fig. 2(e) and (f) show the schematic diagrams of the cross section and top view of the the proposed Si_3N_4 waveguide, respectively. Note that the width differences in Fig. 2(f) are exaggerated for clarity. Each segment consists of a uniform spiral waveguide which helps to save the chip area and n is the number of the segment.

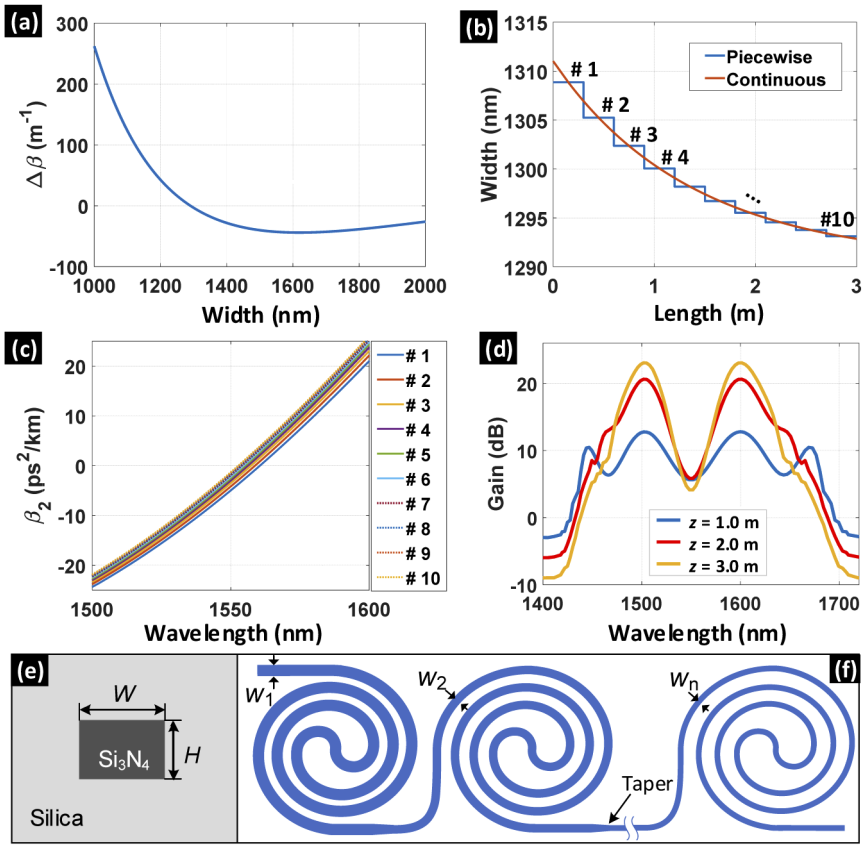

Fig. 2. (a) Intrinsic $\Delta\beta$ of TE_{00} mode changes with the width of the uniform Si_3N_4 waveguide. The pump and the signal wavelengths are 1550 nm and 1600 nm, respectively. $h = 700$ nm. The inset shows the local curve for width between 1280 nm and 1320 nm. (b) The calculated width varying with the Si_3N_4 waveguide length in the case of $\gamma = 1.0$ $m^{-1}W^{-1}$, $\alpha = 3.0$ dB/m and $P_0 = 35.4$ dBm. Red and blue lines are for continuous and piecewise tapers, respectively. (c) β_2 as a function of wavelength for different Si_3N_4 waveguide segments. (d) Simulated gain spectra of tapered Si_3N_4 waveguide OPAs with lengths of 1.0 m (blue line), 2.0 m (red line) and 3.0 m (yellow line), respectively. Schematic diagrams of the (e) cross section and (f) top view of the long Si_3N_4 waveguide. The width of each spiral waveguide is uniform and the width differences in Fig. 2(f) are exaggerated for clarity. The short taper connecting adjacent spiral waveguides is adiabatic.

Optics EXPRESS

3. Simulation results and analysis

In this section, the properties of tapered Si_3N_4-waveguide OPAs with a PG wavelength at 1600 nm are systematically investigated. The taper has a decreasing width and a fixed 700 nm height. The nonlinear coefficient of the waveguide is 1.0 $m^{-1}W^{-1}$.

3.1. Peak gain and variation of PG wavelength

The PG wavelength and the peak gain of the proposed tapered Si_3N_4-waveguide OPAs are investigated in this section. Figure 3(a) shows the PG wavelengths (orange lines) and the peak gain (blue lines) of Si_3N_4-waveguide OPAs with various lengths in the case of $\alpha = 3.0$ dB/m and $P_0 = 35.4$ dBm. Piecewise tapers with ten segments are utilized. The solid lines correspond to the tapered Si_3N_4-waveguide OPA and the dashed lines are for the OPA with a uniform waveguide width of 1310 nm. As can be seen, the PG wavelength of the tapered OPA is constant near the designed target value, while it is shifted from 1594 nm to 1573 nm for the uniform Si_3N_4 waveguide when the waveguide length changes from 0.6 m to 5.0 m. It verifies that the approach of tapering the waveguide width can work well to compensate for the shift of phase matching due to nonnegligible pump attenuation. Moreover, the gain of Si_3N_4-waveguide OPA is the net gain that accounts for the linear loss at the signal wavelength and can be described as

$$G_{\mathrm{Net}}(\mathrm{dB}) = G_{\mathrm{OPA}}(\mathrm{dB}) - Loss(\mathrm{dB}) = G_{\mathrm{OPA}}(\mathrm{dB}) - \alpha z(\mathrm{dB}). \tag{3}$$

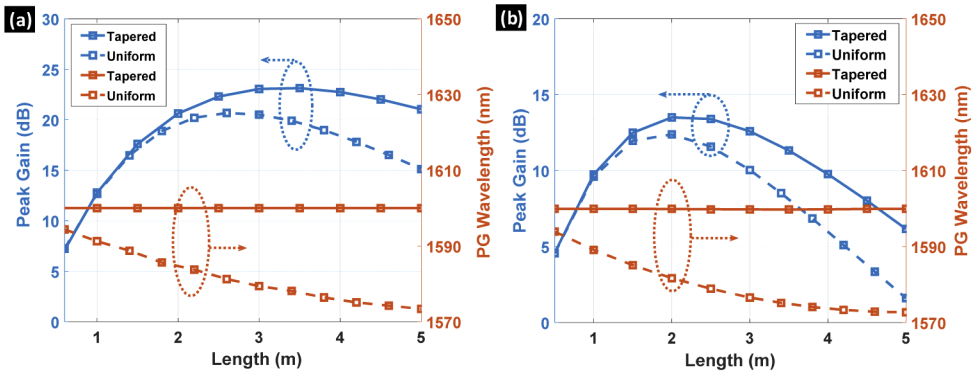

Fig. 3. Evolution of peak gain (blue lines) and PG wavelength (orange lines) of Si_3N_4-waveguide OPAs with different lengths. Solid and dashed lines correspond to the tapered and the uniform waveguides, respectively. The propagation losses are (a) 3.0 dB/m and (b) 4.0 dB/m. P_0 is 35.4 dBm. The width of the uniform Si_3N_4 waveguide is 1310 nm.

The propagation loss leads to the attenuation of the pump, causing a decrease of parametric gain. Moreover, it results in the attenuation of the amplified signal as well. As a result, there is a maximum value of the output peak gain. The slope of the peak gain of the OPA drops with the length of the waveguide. The maximum peak gain of the tapered OPA is 2.5 dB higher than that of the uniform one. In addition, the required length of the Si_3N_4 waveguide to achieve a peak gain of 20.7 dB is 0.6 m (23%) shorter when using the taper. This will help to improve the fabrication yield of long Si_3N_4 waveguides. Figure 3(b) shows the peak gain and the PG wavelengths of integrated Si_3N_4-waveguide OPAs with various lengths when α is 4.0 dB/m. The width is adjusted based on the tapering approach proposed. In this case, the PG wavelength is also well conserved for tapered Si_3N_4-waveguide OPAs with different lengths. Due to the increase of waveguide loss, the maximum parametric gain of both uniform and tapered waveguide OPAs drops. The improvement in peak gain of 1.2 dB is still obtained by using the taper. To achieve

Optics EXPRESS

the same peak gain of 12.4 dB, the length of the tapered Si_3N_4 waveguide is about 1.5 m while it is 2.0 m for the uniform Si_3N_4 waveguide, that is, approximate 25% reduction in length of Si_3N_4 waveguide can be realized. These results are in good agreement with the principle and illustrate the effectiveness of the proposed approach of improving the parametric amplification in Si_3N_4 waveguides.

3.2. Bandwidth

The bandwidth of the integrated Si_3N_4-waveguide OPA was also studied. The pump power is set to be 35.4 dBm. All the Si_3N_4 waveguides are 3.0 m long. The tapered Si_3N_4 waveguides with different losses consist of 10 segments. Figure 4(a) depicts the simulated spectra of different Si_3N_4-waveguide OPAs. The red solid curve is the gain spectrum of the tapered Si_3N_4-waveguide OPA. The widths of the first, the middle and the last segments are 1309 nm, 1298 nm and 1293 nm, respectively. The spectra of uniform Si_3N_4-waveguide OPAs with these three typical widths are also plotted in Fig. 4(a). The blue, red and green dotted lines correspond to the waveguide widths of 1309 nm, 1298 nm and 1293 nm, respectively. As can be seen, the bandwidth of the tapered Si_3N_4-waveguide OPA is widest in the positive net parametric gain regime. The 10 dB bandwidth of the tapered Si_3N_4-waveguide OPA exhibiting the highest peak gain at about 130 nm is slightly narrower than that (about 150 nm) of the uniform 1298 nm-wide-Si_3N_4-waveguide OPA, for which the flat-top spectral shape is attributed to higher-order dispersion [34]. The reason why the peak gain (14.7 dB) of 1293 nm-wide-Si_3N_4-waveguide OPA does not reach that (20.4 dB) of the other two uniform-Si_3N_4-waveguide OPAs is that the perfect phase matching is not achieved. In the case of $\alpha = 4.0$ dB/m, the width of the tapered waveguide changes according to the method proposed to maintain the phase matching condition for a PG wavelength of 1600 nm. The simulated spectra of the tapered (solid line) and the uniform (dotted lines) Si_3N_4-waveguide OPAs are shown in Fig. 4(b). The blue, red and green dotted lines correspond to the waveguide widths of 1308 nm, 1296 nm and 1292 nm, respectively. For the 1308 nm and 1296 nm uniform waveguides, they have effective 10 dB bandwidths of 90 nm and 157 nm, respectively. As can be seen, the tapered OPA has not only the highest net peak gain but also a wide 10 dB bandwidth (148 nm) compared with the uniform-1296 nm-wide-Si_3N_4-waveguide OPAs.

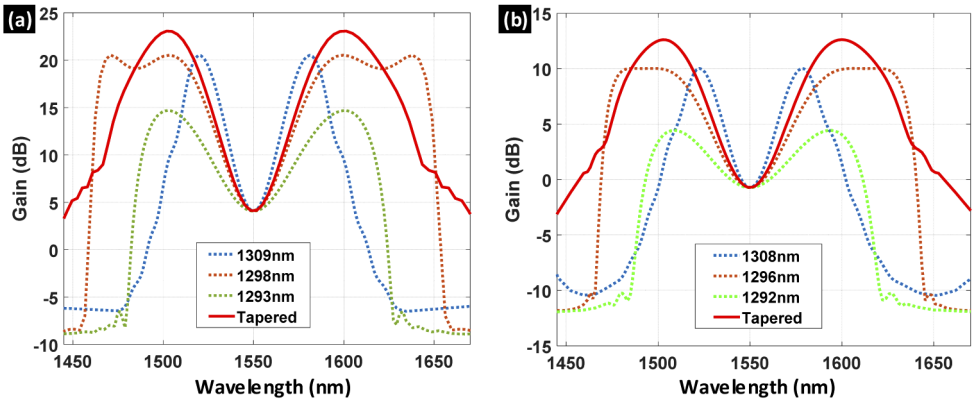

Fig. 4. Simulated net-gain spectra of 3 m-long tapered Si_3N_4-waveguide OPAs with various segments. The solid blue, red, oringe, purple, green and dotted blue lines correpsond to the segment number of 1, 2, 3, 4, 5 and 100, respectively. P_0 is 35.4 dBm. The propagation losses are (a) 3.0 dB/m and (b) 4.0 dB/m, respectively.

Optics EXPRESS

3.3. Segment number dependence

Here the impact of the segment number of the tapered waveguide is investigated, and Fig. 5 shows the simulated gain spectra of tapered Si_3N_4-waveguide OPAs with various segment numbers. The total lengths of the tapers and uniform waveguides are the same (3 m) and the input pump power is 35.4 dBm. The solid blue, red, orange, purple, green and dotted blue lines correspond to the segment number of 1, 2, 3, 4, 5 and 100, respectively. The propagation loss in Fig. 5(a) and (b) is 3.0 dB/m and 4.0 dB/m, respectively. As can be seen in Fig. 5(a), the PG wavelength is almost the same when the segment number increases, even for the one-segment taper which is a uniform waveguide. This validates the proposed method of designing a Si_3N_4-waveguide OPA with specific operation wavelengths. Besides, two segments can lead to a 1.9 dB increase in peak OPA gain. Four segments can achieve about 2.5 dB additional gain compared with the uniform-Si_3N_4-waveguide OPA. Further increase in the sections of the waveguide improves the peak gain little and almost does not affect the OPA spectrum. In the case of $\alpha = 4.0$ dB/m, as shown by Fig. 4(b), the trend is almost the same as illustrated in Fig. 4(a). When the segment number is larger than four, the peak gain of the proposed Si_3N_4-waveguide OPA increases little and the effective bandwidth rarely changes. The bandwidth of the tapered Si_3N_4-waveguide OPA is always broader than that of the uniform one. This indicates that the tapering technique may show more improvements in the performance of Si_3N_4-waveguide OPA when the propagation loss is high.

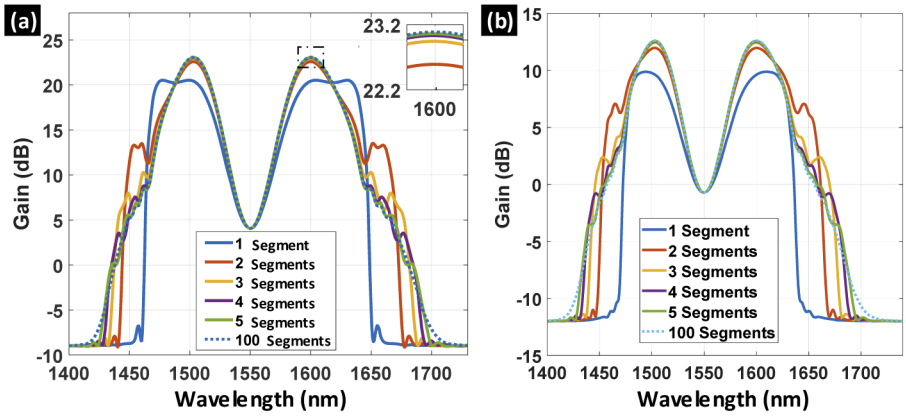

Fig. 5. Gain spectra of tapered (solid lines) and uniform (dotted lines) Si_3N_4-waveguide OPAs with different propagation losses. The lengths of all Si_3N_4 waveguides are 3.0 m. P_0 is 35.4 dBm. (a) $\alpha = 3.0$ dB/m. The widths of the uniform waveguides are 1309 nm (blue dotted), 1298 nm (red dotted) and 1293 nm (green dotted), respectively. (b) $\alpha = 4.0$ dB/m. The widths of the uniform waveguides are 1308 nm (blue dotted), 1296 nm (red dotted) and 1292 nm (green dotted), respectively.

3.4. Pump power dependence

Figure 6 shows the gain spectra of Si_3N_4-waveguide OPAs with different input pump powers. The solid and the dotted lines are the spectra of the tapered and the uniform waveguide OPAs, respectively. The propagation loss of the waveguide is 4.0 dB/m. The lengths of both Si_3N_4 waveguides are 3.0 m. The tapered Si_3N_4 waveguide is composed of 4 segments and designed to have a PG wavelength of 1600 nm with an incident pump power of 35.4 dBm. The blue, red, orange, purple, green and light blue lines are for the cases of P_0 increased from 34.8 dBm to 35.8 dBm with a step of 0.2 dB, respectively. During the change of initial pump power, the width of tapered Si_3N_4 waveguide does not change. In this manner, the influence of pump power on

Optics EXPRESS

the performance of the proposed Si_3N_4-waveguide OPA is investigated. As can be seen, the peak gain of the tapered OPA is always higher than that of the uniform one for the same P_0. The differences in the parametric gain between the target 1600 nm and the PG wavelengths are less than 0.2 dB for the 1 dB variation of pump power. This demonstrates that this technique has a good tolerance for the pump power variation. Besides, the increase in the peak gain from tapering the width of the Si_3N_4 waveguide is 1.9 dB for $P_0 = 34.8$ dBm and reaches 3.5 dB for $P_0 = 35.8$ dBm. This shows that the improvement can be enhanced when the pump power becomes higher.

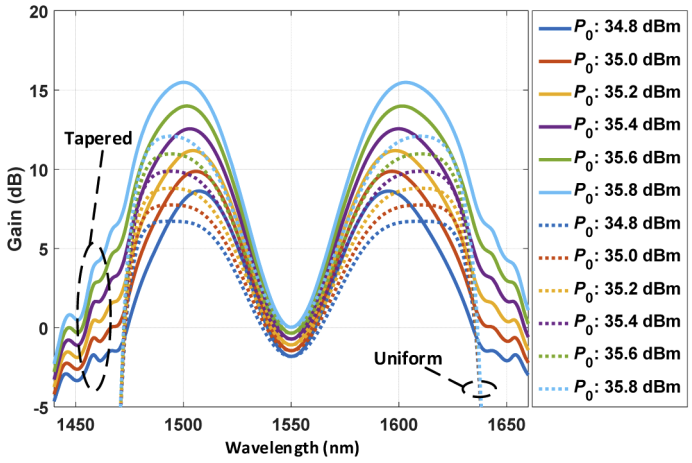

Fig. 6. Spectra of tapered (solid lines, 4 segments) and uniform (dotted lines) 3 m-long Si_3N_4-waveguide OPAs with various input pump powers and $\alpha = 4.0$ dB/m. The PG wavelengths of both the taper and the uniform Si_3N_4-waveguide OPAs are designed to be 1600 nm with $P_0 = 35.4$ dBm. The blue, red, orange, purple, green and light blue lines are for the cases of $P_0 = 34.8$ dBm, 35.0 dBm, 35.2 dBm, 35.4 dBm, 35.6 dBm and 35.8 dBm, respectively.

4. Discussions

In the case of $h = 700$ nm, $\alpha = 3.0$ dB/m and $P_0 = 35.4$ dBm, the improved broadband tapered Si_3N_4-waveguide OPA can have four segments with widths around 1300 nm (1305 nm, 1297 nm, 1294 nm and 1292 nm) in which regime the intrinsic negative $\Delta\beta$ increases with decreased waveguide width. The minimum difference in the waveguide width is 2 nm, which poses challenges for fabrication. It is important to design the width with higher fabrication tolerance. As it can be seen in Fig. 2(a), the modification of $\Delta\beta$ may also be realized by increasing the waveguide width according to the trend of the curve. The slope of $\Delta\beta$ is smaller in this width regime. This indicates that the difference in the width of the tapered Si_3N_4 waveguide will be larger and improves the fabrication tolerance. To achieve perfect phase matching in this regime, the width of the 700 nm-high Si_3N_4 waveguide will be much larger than 2000 nm, which would increase the risk of exciting higher-order modes.

Reducing the height of the Si_3N_4 waveguide can facilitate to reach this goal. Figure 7(a) shows the $\Delta\beta$ of TE_{00} mode varying with the width for a 680 nm thick Si_3N_4 waveguide. The pump wavelength is 1550 nm and the target PG wavelength of this OPA is 1640 nm. As can be seen, $\Delta\beta$ of approaches zero for widths around1420 nm and 2000 nm. The 2000 nm-width regime is more suitable to taper the Si_3N_4 waveguide for the improvement of parametric amplification. With the approach proposed, the calculated width along the piecewise quasi-continuously-tapered Si_3N_4 waveguide is shown by the blue curve in Fig. 7(b) in the case of $P_0 = 35.4$ dBm and $\alpha = 3.0$ dB/m. The nonlinear coefficient is 1.0 $m^{-1}W^{-1}$. The widths of the four segments are 1965 nm, 1976

Optics EXPRESS

nm, 1982 nm and 1986 nm, respectively. The difference in waveguide width is feasible with the advance of nano-fabrication technologies [35]. We also performed simulations where there are some variations of waveguide width in the case of fabrication accuracy of 2 nm. We find that the peak gain of this tapered Si_3N_4-waveguide OPA is still 1.8 dB higher than that of uniform one. Each segment can be easily shaped into widely-used spiral waveguides to achieve a balance between length and area [36,37]. The red line in Fig. 7(c) shows the simulated gain spectrum of the tapered OPA. In contrast, the blue line is a spectrum of a uniform Si_3N_4-waveguide OPA with a width of 1980 nm. It is clear that the improved tapered OPA not only has a 2.5 dB higher peak gain but also exhibits broader bandwidth. The 10 dB bandwidth can be up to 172 nm and the bandwidth for positive parametric gain is even more than 260 nm in the case of a single CW pump. These properties make the proposed integrated Si_3N_4 OPA promising in broadband optical signal processing.

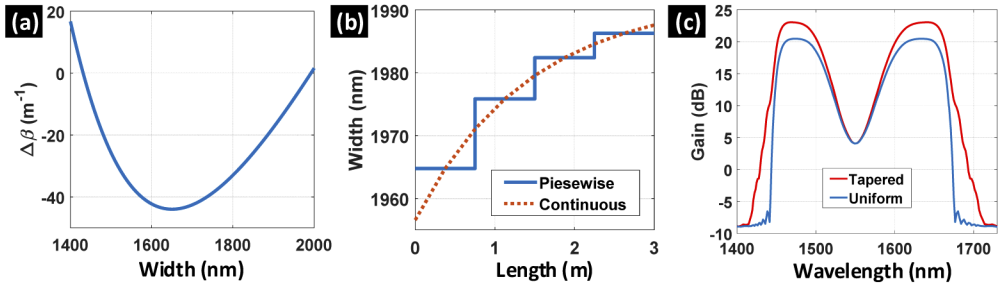

Fig. 7. (a) Intrinsic $\Delta\beta$ of TE_{00} mode varying with the width of the Si_3N_4 waveguide with $h = 680$ nm. The pump and signal wavelenths are 1550 nm and 1640nm, respectively. (b) The calculated width along the Si_3N_4 waveguide. Red dotted and blue lines are for continuous and piecewise tapers, respectively. γ is 1.0 $m^{-1}W^{-1}$, $\alpha = 3.0$ dB/m and $P_0 = 35.4$ dBm. (c) Simulated gain spectra of tapered (red) and uniform (blue) Si_3N_4-waveguide OPAs.

5. Summary

In summary, improving the parametric amplification in integrated Si_3N_4 OPAs by tapering the waveguide width is proposed and systematically investigated in this paper. This technique can effectively boost the performance of OPAs with lossy Si_3N_4 waveguides, which is verified by simulations based on NLSE. According to the simulation results, peak parametric gain at precise target wavelengths is realized in spite of the variation of waveguide length. In addition, the length of the tapered Si_3N_4 waveguide can be reduced for the integrated OPA to reach the same maximum peak gain of the OPA with a single uniform Si_3N_4 waveguide. Besides, the tapered Si_3N_4-waveguide OPA also exhibits broadband operation. It is found that piecewise tapers with four sections can reach similar performance as a continuous taper. This indicates that the fabrication of the proposed integrated OPA can be simplified. Besides, decreasing or increasing the width can both work and increasing it can lead to more tolerance to fabrication. The proposed tapered integrated Si_3N_4 OPAs offer potential for a wide range of applications in optical communications, optical signal processing and microwave photonics.

Funding

Swedish Research Council (VR) (2015-00535).

Optics EXPRESS

Acknowledgements

The authors thank Prof. Victor Torres-Company, Dr. Fuchuan Lei and Dr. Francisco Rodrigo Arteaga Sierra for their discussions.

Disclosures

The authors declare no conflicts of interest.

References

1. J. Hansryd, P. A. Andrekson, M. Westlund, J. Li, and P.-O. Hedekvist, "Fiber-based optical parametric amplifiers and their applications," IEEE J. Sel. Top. Quantum Electron. **8**(3), 506–520 (2002).
2. Z. Tong, C. Lundström, P. A. Andrekson, C. J. McKinstrie, M. Karlsson, D. J. Blessing, E. Tipsuwannakul, B. J. Puttnam, H. Toda, and L. Grüner-Nielsen, "Towards ultrasensitive optical links enabled by low-noise phase-sensitive amplifiers," Nat. Photonics **5**(7), 430–436 (2011).
3. R. Slavík, F. Parmigiani, J. Kakande, C. Lundström, M. Sjödin, P. A. Andrekson, R. Weerasuriya, S. Sygletos, A. D. Ellis, L. Grüner-Nielsen, D. Jakobsen, S. Herstrøm, R. Phelan, J. O'Gorman, A. Bogris, D. Syvridis, S. Dasgupta, P. Petropoulos, and D. J. Richardson, "All-optical phase and amplitude regenerator for next-generation telecommunications systems," Nat. Photonics **4**(10), 690–695 (2010).
4. R. Slavík, J. Kakande, P. Petropoulos, and D. J. Richardson, "Processing of optical combs with fiber optic parametric amplifiers," Opt. Express **20**(9), 10059–10070 (2012).
5. C. Bao, Y. Yan, L. Zhang, Y. Yue, N. Ahmed, A. M. Agarwal, L. C. Kimerling, J. Michel, and A. E. Willner, "Increased bandwidth with flattened and low dispersion in a horizontal double-slot silicon waveguide," J. Opt. Soc. Am. B **32**(1), 26–30 (2015).
6. J. Li, K. K. Y. Cheung, and K. K. Y. Wong, "Photonic Microwave Filter with Negative Coefficients Using Fiber Optical Parametric Amplifier," in *Optical Fiber Communication Conference and National Fiber Optic Engineers Conference, OSA Technical Digest (CD)* (Optical Society of America, 2009), p. JWA53.
7. K. Yang, J. Jiang, Z. Guo, Q. Hao, and H. Zeng, "Tunable Femtosecond Laser From 965 to 1025 nm in Fiber Optical Parametric Oscillator," IEEE Photonics Technol. Lett. **30**(7), 607–610 (2018).
8. Q. Lin and G. P. Agrawal, "Effects of polarization-mode dispersion on fiber-based parametric amplification and wavelength conversion," Opt. Lett. **29**(10), 1114–1116 (2004).
9. M. A. Foster, A. C. Turner, J. E. Sharping, B. S. Schmidt, M. Lipson, and A. L. Gaeta, "Broad-band optical parametric gain on a silicon photonic chip," Nature **441**(7096), 960–963 (2006).
10. M. R. Lamont, B. Luther-Davies, D.-Y. Choi, S. Madden, X. Gai, and B. J. Eggleton, "Net-gain from a parametric amplifier on a chalcogenide optical chip," Opt. Express **16**(25), 20374–20381 (2008).
11. T. Umeki, O. Tadanaga, A. Takada, and M. Asobe, "Phase sensitive degenerate parametric amplification using directly-bonded PPLN ridge waveguides," Opt. Express **19**(7), 6326–6332 (2011).
12. X. Liu, R. M. Osgood, Y. A. Vlasov, and W. M. J. Green, "Mid-infrared optical parametric amplifier using silicon nanophotonic waveguides," Nat. Photonics **4**(8), 557–560 (2010).
13. D. J. Moss, R. Morandotti, A. L. Gaeta, and M. Lipson, "New CMOS-compatible platforms based on silicon nitride and Hydex for nonlinear optics," Nat. Photonics **7**(8), 597–607 (2013).
14. Y. Xuan, Y. Liu, L. T. Varghese, A. J. Metcalf, X. Xue, P.-H. Wang, K. Han, J. A. Jaramillo-Villegas, A. Al Noman, C. Wang, S. Kim, M. Teng, Y. J. Lee, B. Niu, L. Fan, J. Wang, D. E. Leaird, A. M. Weiner, and M. Qi, "High-Q silicon nitride microresonators exhibiting low-power frequency comb initiation," Optica **3**(11), 1171–1180 (2016).
15. J. Liu, A. S. Raja, M. Karpov, B. Ghadiani, M. H. P. Pfeiffer, B. Du, N. J. Engelsen, H. Guo, M. Zervas, and T. J. Kippenberg, "Ultralow-power chip-based soliton microcombs for photonic integration," Optica **5**(10), 1347–1353 (2018).
16. Z. Ye, K. Twayana, P. A. Andrekson, and V. Torres-Company, "High-Q Si3N4 microresonators based on a subtractive processing for Kerr nonlinear optics," Opt. Express **27**(24), 35719–35727 (2019).
17. M. Karpov, H. Guo, A. Kordts, V. Brasch, M. H. P. Pfeiffer, M. Zervas, M. Geiselmann, and T. J. Kippenberg, "Raman Self-Frequency Shift of Dissipative Kerr Solitons in an Optical Microresonator," Phys. Rev. Lett. **116**(10), 103902 (2016).
18. F. Gyger, J. Liu, F. Yang, J. He, A. S. Raja, R. N. Wang, S. A. Bhave, T. J. Kippenberg, and L. Thévenaz, "Observation of Stimulated Brillouin Scattering in Silicon Nitride Integrated Waveguides," Phys. Rev. Lett. **124**(1), 013902 (2020).
19. A. Klenner, A. S. Mayer, A. R. Johnson, K. Luke, M. R. E. Lamont, Y. Okawachi, M. Lipson, A. L. Gaeta, and U. Keller, "Gigahertz frequency comb offset stabilization based on supercontinuum generation in silicon nitride waveguides," Opt. Express **24**(10), 11043–11053 (2016).
20. X. Ji, F. A. S. Barbosa, S. P. Roberts, A. Dutt, J. Cardenas, Y. Okawachi, A. Bryant, A. L. Gaeta, and M. Lipson, "Ultra-low-loss on-chip resonators with sub-milliwatt parametric oscillation threshold," Optica **4**(6), 619–624 (2017).
21. X. Xue, Y. Xuan, C. Wang, P.-H. Wang, Y. Liu, B. Niu, D. E. Leaird, M. Qi, and A. M. Weiner, "Thermal tuning of Kerr frequency combs in silicon nitride microring resonators," Opt. Express **24**(1), 687–698 (2016).

Optics EXPRESS

22. C.-L. Tien and T.-W. Lin, "Thermal expansion coefficient and thermomechanical properties of SiNx thin films prepared by plasma-enhanced chemical vapor deposition," Appl. Opt. **51**(30), 7229–7235 (2012).
23. H. El Dirani, L. Youssef, C. Petit-Etienne, S. Kerdiles, P. Grosse, C. Monat, E. Pargon, and C. Sciancalepore, "Ultralow-loss tightly confining Si3N4 waveguides and high-Q microresonators," Opt. Express **27**(21), 30726–30740 (2019).
24. Y. Zhang, J. Schroeder, C. Husko, S. Lefrancois, D.-Y. Choi, S. Madden, B. Luther-Davies, and B. J. Eggleton, "Pump-degenerate phase-sensitive amplification in chalcogenide waveguides," J. Opt. Soc. Am. B **31**(4), 780–787 (2014).
25. K. Tajima, "Compensation of soliton broadening in nonlinear optical fibers with loss," Opt. Lett. **12**(1), 54–56 (1987).
26. S. V. Chernikov, E. M. Dianov, D. J. Richardson, and D. N. Payne, "Soliton pulse compression in dispersion-decreasing fiber," Opt. Lett. **18**(7), 476–478 (1993).
27. A. C. Peacock, "Soliton propagation in tapered silicon core fibers," Opt. Lett. **35**(21), 3697–3699 (2010).
28. S. Lavdas, J. B. Driscoll, H. Jiang, R. R. Grote, R. M. Osgood, and N. C. Panoiu, "Generation of parabolic similaritons in tapered silicon photonic wires: comparison of pulse dynamics at telecom and mid-infrared wavelengths," Opt. Lett. **38**(19), 3953–3956 (2013).
29. J. Yuan, J. Chen, F. Li, C. Mei, Z. Kang, X. Zhang, Y. Xu, B. Yan, X. Sang, Q. Wu, X. Zhou, K. Zhong, K. Wang, C. Yu, G. Farrell, and P. K. A. Wai, "Mid-infrared self-similar compression of picosecond pulse in an inversely tapered silicon ridge waveguide," Opt. Express **25**(26), 33439–33450 (2017).
30. T. Lee, Y. Jung, C. A. Codemard, M. Ding, N. G. R. Broderick, and G. Brambilla, "Broadband third harmonic generation in tapered silica fibres," Opt. Express **20**(8), 8503–8511 (2012).
31. Z. Wang, H. Liu, Q. Sun, N. Huang, and X. Li, "Frequency non-degenerate phase-sensitive optical parametric amplification based on fourwave-mixing in width-modulated silicon waveguides," Opt. Express **22**(25), 31486–31495 (2014).
32. G. Agrawal, *Nonlinear Fiber Optics* (Academic, 2013).
33. X. Ji, X. Yao, Y. Gan, A. Mohanty, M. A. Tadayon, C. P. Hendon, and M. Lipson, "On-chip tunable photonic delay line," APL Photonics **4**(9), 090803 (2019).
34. M. E. Marhic, *Fiber Optical Parametric Amplifiers, Oscillators and Related Devices* (Cambridge University, 2007).
35. https://www.tsmc.com/download/ir/annualReports/2018/english/pdf/2018_tsmc_ar_e_ch1.pdf.
36. F. Da Ros, E. Porto da Silva, D. Zibar, S. T. Chu, B. E. Little, R. Morandotti, M. Galili, D. J. Moss, and L. K. Oxenløwe, "Wavelength conversion of QAM signals in a low loss CMOS compatible spiral waveguide," APL Photonics **2**(4), 046105 (2017).
37. Y. Li, K. Zhu, Z. Kang, W. L. Ho, R. Davidson, C. Lu, B. E. Little, and S. T. Chu, "CMOS-compatible high-index doped silica waveguide with an embedded silicon-nanocrystal strip for all-optical analog-to-digital conversion," Photonics Res. **7**(10), 1200–1208 (2019).